THE UNIVERSITY OF NORTHAMPTON

This work has been submitted to NECTAR, the Northampton Electronic Collection of Theses and Research.

Article

Title: Control of actuators for cabin vibration damping of a rope-free passenger transportation system

Creators: Missler, J., Ehrl, T., Meier, B., Kaczmarczyk, S. and Sawodny, O.

Example citation: Missler, J., Ehrl, T., Meier, B., Kaczmarczyk, S. and Sawodny, O. (2017) Control of actuators for cabin vibration damping of a rope-free passenger transportation system. *Lift and Escalator Symposium.* **7**, 16/1-16/11. 2052-7225.

It is advisable to refer to the publisher's version if you intend to cite from this work.

Version: Published version

Official URL:
https://liftsymposium.org/download/LiftandEscalatorSymposiumProceedings2017.pdf

http://nectar.northampton.ac.uk/9923/

Control of Actuators for Cabin Vibration Damping of a Rope-Free Passenger Transportation System

Jonas Missler[1], Thomas Ehrl[2], Benedikt Meier[2], Stefan Kaczmarczyk[3] and Oliver Sawodny[1]

[1]Institute for System Dynamics (ISYS), University Stuttgart, Waldburgstr. 19, 70563 Stuttgart, Germany, Email: missler@isys.uni-stuttgart.de, sawodny@isys.uni-stuttgart.de
[2]thyssenkrupp Elevator Innovation GmbH, Berner Feld 60, 78628 Rottweil, Germany, Email: thomas.ehrl@thyssenkrupp.com, benedikt.meier@thyssenkrupp.com
[3]Faculty of Arts, Science and Technology, University of Northampton, St. George's Avenue, Northampton NN7 3NG, UK, Email: stefan.kaczmarczyk@northampton.ac.uk

Keywords: Vibration Damping, Control Engineering, Dynamic Modelling, Disturbance Estimation

Abstract. The design of the novel rope-free passenger transportation system (PTS) differs from that of conventional traction lifts. The new propulsion, realized through a linear motor, requires lightweight constructions and thus shapes the design of the PTS. Additionally the possibility of horizontal travel has great influence on the difference between the design of conventional traction lifts and the PTS. Despite the different design, the aim for the rope-free PTS is to achieve at least the same ride quality as modern traction lifts. One important point in achieving the required ride quality is to reduce the vibrations felt by the passengers inside the cabin. In general, the damping concepts of conventional lifts cannot be readily applied to the new design of the PTS. Therefore, a damping concept for the rope-free PTS has to be developed. This paper will present the possibilities of active vibration damping for the PTS and a possible actuator position. The paper will focus on the modelling of the active damping components and the control of actuators deployed in the system. The performance of the damping actuators will be evaluated using a simulation with a Multi-Body System (MBS) of the PTS. The primary disturbance of the PTS for this paper will be the vibrations induced by the guidance.

1 INTRODUCTION

The rope-free PTS introduces a novel form of vertical transportation by eliminating the rope from the propulsion system. The propulsion of the PTS replaces the rope and the rotational motor by a linear motor, which directly provides the vertical driving force for the car of the PTS. The linear motor enables the simultaneous movement of multiple cars in a single shaft and makes horizontal travel possible. The new propulsion also demands a new lift design that differs from the design of conventional traction lifts. The car of the rope-free PTS consists of three main components: the sledge with the passive elements of the linear motor, the mounting frame for the cabin, and the actual cabin. The active components, thus the coil units, of the linear motor are placed in the shaft wall. The Fig. 1 shows a sketch of the rope-free PTS and its three main components. The design of the PTS omits the mounting frame around the cabin, which is used in standard lifts to decouple the motion of the cabin from the rest of the car and therefore provides good riding comfort. The omission of the frame around the cabin enables an easy realization of horizontal and vertical travel in a single system, but also reduces the ability to damp vibrations in the rope-free PTS. In order to achieve a similar riding comfort as in conventional lifts an active vibration damping is designed for the rope-free PTS. This paper will present a control scheme for active vibration damping of the rope-free PTS, which is based on the disturbance estimation and compensation. The compensation is based on the system inversion will be shown briefly.

In general, the active vibration damping task can be viewed as the rejection of undesired behaviour of the system. This undesired behaviour is in many cases caused by some external source such as deflections in the guidance system. This external source can be modelled as a disturbance input to the system. The problem with the disturbance, that shall be compensated, is that often the

disturbance is not directly measureable at the real system. Therefore, the disturbance causing the vibrations has to be estimated, so it can be directly compensated. The estimation of disturbances is a common field in the control theory, and many different techniques exist to derive a disturbance estimator [1]. One technique for disturbance estimation augments is the model of the real system with a model of a disturbance generator [2]. In the simplest case, this model is chosen to be zero to estimate a constant disturbance. Finding the optimal observer under certain condition is often done by minimizing a quadratic objective related to the model of the plant for which it is design leading to a linear quadratic estimator, the well-known Kalman-Filter [3]. There also exist many different disturbance rejection controllers, which rely on much less knowledge of the system dynamics [4], the controllers can be implemented without deriving a model of the system. The disturbance rejection control was also already implemented on an under actuated MBS in [5], which describes systems with more degrees of freedom (DOF) than independent control inputs.

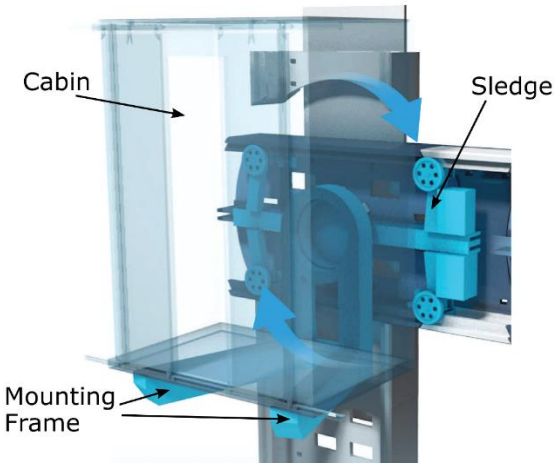

Figure 1 Rope-free passenger transportation system (PTS) in exchanger position.
Source: multi.thyssenkrupp-elevator.com

The modelling of the rope-free PTS was performed using the internationally standardized method of Multi-Body Systems (MBS). The method of MBS is especially useful in the context of rigid system undergoing large rotational and translational displacements. The MBS method is part of classical mechanical engineering [6]. The in this paper used model is a variant of the model presented earlier [7]. The disturbance estimation and compensation in this paper is based on the linearization of the MBS. The linearization of a system is a widely used technique for deriving a controller or observer for a nonlinear system [8], especially if the relevant motion of the system stays in a small range around the desired motion of the system.

The compensation mechanism will only be discussed briefly in this paper. The used compensation is based on the control of under actuated MBS. The technique for the control of under actuated MBS is described in [9], and is based on the well-known technique of input/output linearization for nonlinear systems [10, 11]. The advantage of the control of under actuated MBS is that it can be directly applied to the dynamic equations of MBS. As mentioned in [9] the main computational disadvantage of the control of under actuated MBS is that the non-actuated part of the MBS has to be simulated alongside the inversion of the system.

The fact that the disturbance will never be perfectly estimated also makes it necessary to implement a stabilizing feedback together with the disturbance compensation. The implementation of such a stabilizing controller will not be in the scope of this paper. The paper is structured in the following fashion. First, the nonlinear model used for the design of the estimator and disturbance compensation is described. The following chapter will display the design of the disturbance estimation and briefly sketch the design of the disturbance compensation. The fourth chapter will

give a simulation example based on the model derived in the second chapter. The last chapter will conclude the paper and give an outlook on the possible extension of the disturbance compensation.

2 MODEL

The principle two-dimensional model used in this paper is the same as in [7]. The difference in the model is that the actuators underneath the cabin in the model were replaced by a single actuator, that can apply a force in the z-direction and a torque around the y-axes underneath the cabin. Therefore, the two forces F_{A1} and F_{A2} from the actuators are replaced by a single force F_C and a torque T_C underneath the cabin, see Fig. 2. The omission of the closed kinematic loop has the main advantage that the resulting model of the PTS is in tree structure, which is better suited for controller or observer design, due to the more simple structure. It is important to note that the new model only approximates the motion of the two parallel actuators, because the single actuator reduces the DOF of the model by one resulting in five degrees of freedom. The reduction in the DOF restricts the relative motions that run purely parallel to the x-axis of the cabin. This restriction in x-direction will not play a big role, because for the control design the relative motion in x-direction cannot be effectively damped by two parallel actuators underneath the cabin, which both face in z-direction. The reduction in generalised coordinates, by the reduction from two actuators underneath the cabin to a single one is also displayed in Fig. 2. The transformation between the new and old generalised coordinates can be approximated by

$$\begin{bmatrix} x_c \\ z_c \\ \beta_c \end{bmatrix} \approx \begin{bmatrix} \begin{bmatrix} x_b \\ z_b \end{bmatrix} + \begin{bmatrix} \sin(\beta_b + \varphi_c) \\ \cos(\beta_b + \varphi_c) \end{bmatrix} r_c + \begin{bmatrix} \cos(\beta_b) & \sin(\beta_b) \\ -\sin(\beta_b) & \cos(\beta_b) \end{bmatrix} \boldsymbol{r}_{B0}^{Cb} \\ \beta_b + \varphi_c \end{bmatrix}. \tag{1}$$

The transformation from the two actuators in parallel to the single actuator with force and torque can be performed using

$$F_C = [\cos(\beta_1)\ \cos(\beta_2)] \begin{bmatrix} F_{A1} \\ F_{A2} \end{bmatrix}, \qquad T_C = \sum_{i=1}^{2} [d_{z,i}\ -d_{x,i}] \begin{bmatrix} \sin(\beta_i) \\ \cos(\beta_i) \end{bmatrix} F_{A,i}, \tag{2}$$

where β_1 and β_2 are the respective angles of the actuators A_1 and A_2, they can be calculated from the closing condition of the original two-dimensional model. The distances $d_{z,i}, d_{x,i}$ are the distances from the contact P_i of the actuators to the point P_0, thus $\boldsymbol{r}_{Pi}^{P0} = [d_{x,i}\ \ d_{z,i}]^T,\ i = 1,2$.

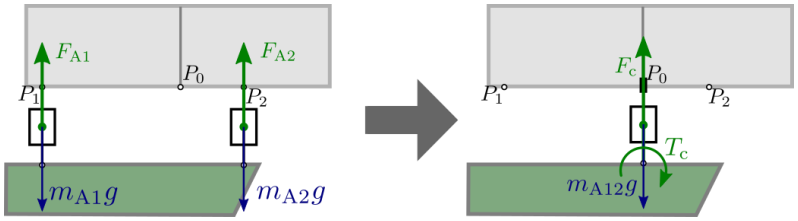

Figure 2 Reduction DOF by replacing the closed loop. The two parallel actuators in the model are replaced by a single actuator, which can apply the force F_C and the torque T_C.

The model can be rewritten with the new generalised coordinates $\boldsymbol{q} = [x_b, z_b, \beta_b, r_c, \varphi_c]^T \in \mathbb{R}^f$ with the DOF $f = 5$ in the standard form of MBS given by

$$\boldsymbol{M}(\boldsymbol{q}, t)\ddot{\boldsymbol{q}} + \boldsymbol{k}(\boldsymbol{q}, \dot{\boldsymbol{q}}, t) = \boldsymbol{g}(\boldsymbol{q}, \dot{\boldsymbol{q}}, t), \tag{3}$$

where the matrix $\boldsymbol{M} \in \mathbb{R}^{f \times f}$ is the symmetric mass matrix, $\boldsymbol{k} \in \mathbb{R}^f$ inherits the internal forces, such as spring and damping forces, and $\boldsymbol{g} \in \mathbb{R}^f$ contains the external forces, thus inputs and disturbances. Fig. 3(a) shows the two-dimensional model of the rope-free PTS including the

disturbance force F_d and torque T_d, which convey the vibration from the guiding system through the point B_s to the mounting frame. Additionally, the generalised coordinates $\boldsymbol{q}$ of the system are also shown in the Fig. 3(b).

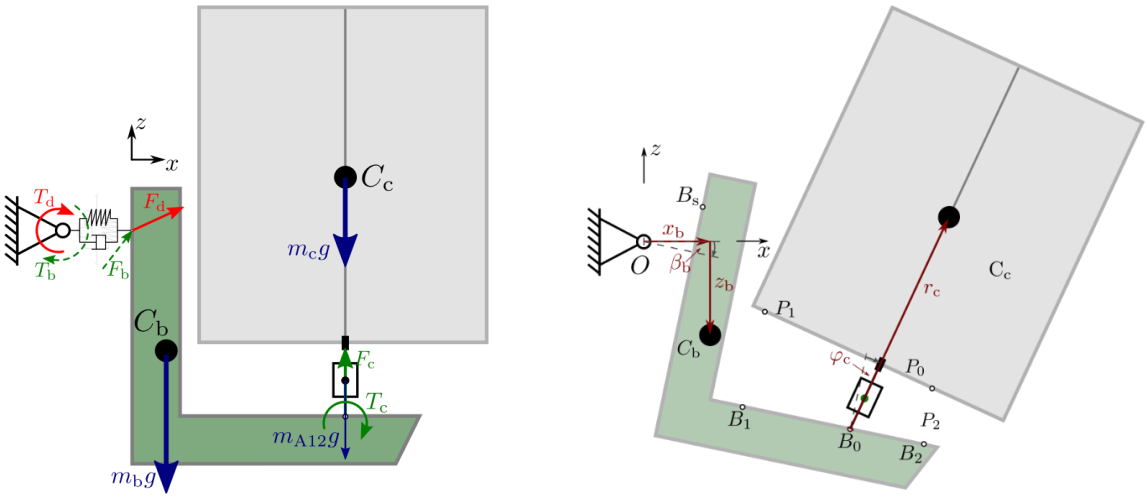

(a) Simplified two-dimensional MBS. **(b) Generalised coordinates.**

Figure 3 Simplified two-dimensional model consisting of mounting frame and cabin. In (a) are the disturbances from the guidance, force F_d and torque T_d. The force F_c and torque T_c represent equivalence for the actuator forces and in blue are the gravitational forces. In (b) the generalised coordinates of the model are displayed, namely $\mathbf{q} = [x_b, z_b, \beta_b, r_c, \varphi_c]^T$.

3 CONTROL CONCEPT

The overall control concept is based on two parts: The disturbance estimation and its compensation. The estimation is necessary because a measurement of the disturbance force F_d and torque T_d is not directly possible. The disturbance is estimated on base of the measurable output signals $\boldsymbol{y}$ and the control input $\boldsymbol{u}$ of the system. The Fig. 4 shows the principle structure of the control concept. The disturbance $\boldsymbol{d}$ of the system is assumed to be a force and torque acting as an additional input on the system, see also Fig. 3. The in Fig. 4 shown state feedback will not be part of this paper.

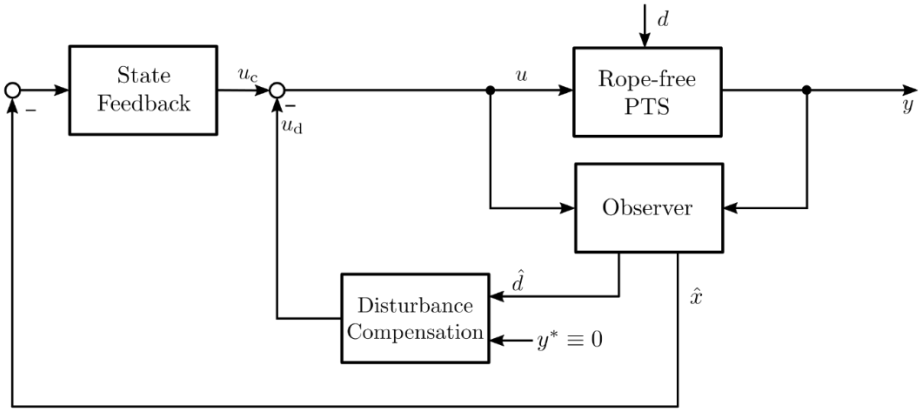

Figure 4 The disturbance compensation structure for the rope-free PTS. The disturbance $\boldsymbol{d} = [F_{dx}, F_{dz}, T_d]^T$ is estimated by $\hat{\boldsymbol{d}}$ and compensated by the input $\boldsymbol{u_d}$.

The disturbance $\boldsymbol{d}$ is the torque and forces acting on the connection point between the bucket and the sledge B_s, thus $\boldsymbol{d} = [F_{dx}, F_{dz}, T_d]^T$. The measureable output is given by

$$\boldsymbol{y} = [x_c, z_c, \beta_c, r_c, \varphi_c]^T = \bar{C} \cdot \bar{\boldsymbol{q}}, \tag{4}$$

where $\bar{C}$ represents

$$\bar{C} = \begin{bmatrix} 1 & 0 & r_c^* - \boldsymbol{r}_{B0}^{Cb}(2) & 0 & r_c^* \\ 0 & 1 & -\boldsymbol{r}_{B0}^{Cb}(1) & 1 & 0 \\ 0 & 0 & 1 & 0 & 1 \\ 0 & 0 & 0 & 1 & 0 \\ 0 & 0 & 0 & 0 & 1 \end{bmatrix}, \tag{5}$$

the generalised coordinates of the linear system $\overline{\boldsymbol{q}}$ describe the small perturbation from the generalised coordinates $\boldsymbol{q}$, thus $\boldsymbol{q} = \boldsymbol{q}^* + \overline{\boldsymbol{q}}$ with the constant steady-state $\boldsymbol{q}^*$. The disturbance $\boldsymbol{d}$ is estimated by $\widehat{\boldsymbol{d}}$ and the state $\boldsymbol{x}$ is estimated by $\widehat{\boldsymbol{x}}$. The control input is the force and torque of the single actuator underneath the cabin $\boldsymbol{u} = [F_c, T_c]$.

In the following, the disturbance and state estimation will be shortly displayed and the rudimentary disturbance compensation used in this paper will be introduced.

3.1 Disturbance and state estimation

The estimation of disturbance $\boldsymbol{d}$ and especially the system state $\boldsymbol{x}$ is a wide field in the control theory and many different estimators exists. This paper will focus on observers that can estimate the state of a system alongside the disturbance, by augmenting, thus extending, the model with a model of the disturbance generator.

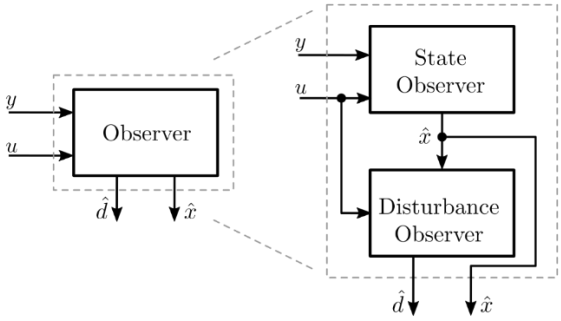

Figure 5 The observer can be split in a state observer, estimating the state $\widehat{\boldsymbol{x}}$, and a disturbance observer, which estimates the disturbance $\widehat{\boldsymbol{d}}$.

The estimator is based on the linearization of the nonlinear model in Chapter 2. The linearization of the MBS, [8, p.108], (3) shall be given by

$$\boldsymbol{M_{lin}}\,\ddot{\overline{\boldsymbol{q}}}(t) + \boldsymbol{P_{lin}}\dot{\overline{\boldsymbol{q}}}(t) + \boldsymbol{Q_{lin}}\overline{\boldsymbol{q}}(t) = \overline{\boldsymbol{B}}_{\boldsymbol{u}}\boldsymbol{u}(t) + \overline{\boldsymbol{B}}_{\boldsymbol{d}}\boldsymbol{d}(t), \tag{6}$$

where $\overline{\boldsymbol{q}}$ are the linearized generalised coordinates, $\boldsymbol{M_{lin}} \in \mathbb{R}^{f\times f}$, $\boldsymbol{P_{lin}} \in \mathbb{R}^{f\times f}$, $\boldsymbol{Q_{lin}} \in \mathbb{R}^{f\times f}$ represent the linearized dynamics of the MBS linearized around the steady-state $\boldsymbol{q}^s = \boldsymbol{q}(t_0)$ and f are the DOF. The matrices $\overline{\boldsymbol{B}}_{\boldsymbol{u}} \in \mathbb{R}^2$ and $\overline{\boldsymbol{B}}_{\boldsymbol{d}} \in \mathbb{R}^3$ are the input matrices for the input $\boldsymbol{u}$ and the disturbance $\boldsymbol{d}$. Using the linear matrices, (6), the system can be written in state-space representation with the state as $\boldsymbol{x} = \left[\overline{\boldsymbol{q}}, \dot{\overline{\boldsymbol{q}}}\right]^T$

$$\dot{\boldsymbol{x}} = A\boldsymbol{x} + B_u\boldsymbol{u} + B_d\boldsymbol{d}; \quad \boldsymbol{y} = C\boldsymbol{x}, \tag{7}$$

where

$$A = \begin{bmatrix} 0 & I \\ -\boldsymbol{M_{lin}^{-1}} \cdot \boldsymbol{Q_{lin}} & -\boldsymbol{M_{lin}^{-1}} \cdot \boldsymbol{P_{lin}} \end{bmatrix},\ B_u = \begin{bmatrix} 0 \\ \boldsymbol{M_{lin}^{-1}} \cdot \overline{\boldsymbol{B}}_{\boldsymbol{u}} \end{bmatrix}, B_d = \begin{bmatrix} 0 \\ \boldsymbol{M_{lin}^{-1}} \cdot \overline{\boldsymbol{B}}_{\boldsymbol{d}} \end{bmatrix},\ C = [\bar{C}\ \ 0]. \tag{8}$$

The measurable output $\boldsymbol{y}$ follows from the assumption, that the motion of the cabin (x_C, z_C, β_C) and additionally the motion of the actuator (r_C, β_C) can be measured. The state-space representation (8) has the advantage that many properties of the system can be checked easily. One property, which has to be checked before the design of an observer, is the observability of the system (7), thus if the state can be reconstructed from the output $\boldsymbol{y}$. For the linearized time invariant system (7) this can be checked by ensuring the rank of the observability matrix $O = [C^T, (C \cdot A)^T]^T$ of the system. The rank of the observability matrix is 10, which corresponds to the number of states of the linear system (7), and therefore the at least the linearized system is observable.

The state-space system (7) will be augmented with an assumed dynamics of the disturbance $\boldsymbol{d}$. Assume that the disturbance is generated by the system

$$\dot{\boldsymbol{x}}_{\boldsymbol{d}} = A_d \boldsymbol{x}_{\boldsymbol{d}} + G\boldsymbol{w}; \quad \boldsymbol{d} = C_d \boldsymbol{x}_{\boldsymbol{d}}, \tag{9}$$

where $\boldsymbol{x}_{\boldsymbol{d}} \in \mathbb{R}^{2 \cdot n_d}$ is the state of the disturbance generator and $\boldsymbol{w} \in \mathbb{R}^{n_d}$ is a white noise disturbance with its respective input matrix $G \in \mathbb{R}^{2 \cdot n_d \times n_d}$, here the number of disturbances $n_d = 3$. The augmented plant consisting of system (7) and (9) is then given by

$$\begin{bmatrix} \dot{\boldsymbol{x}} \\ \dot{\boldsymbol{x}}_{\boldsymbol{d}} \end{bmatrix} = \begin{bmatrix} A & B_d \cdot C_d \\ 0 & A_d \end{bmatrix} \begin{bmatrix} \boldsymbol{x} \\ \boldsymbol{x}_{\boldsymbol{d}} \end{bmatrix} + \begin{bmatrix} B \\ 0 \end{bmatrix} \boldsymbol{u} + \begin{bmatrix} 0 \\ G \end{bmatrix} \boldsymbol{w}; \quad \boldsymbol{y} = [C \quad 0] \begin{bmatrix} \boldsymbol{x} \\ \boldsymbol{x}_{\boldsymbol{d}} \end{bmatrix} + \boldsymbol{\nu}, \tag{10}$$

where $\boldsymbol{\nu} \in \mathbb{R}^5$ is an additional measurement noise. The overall state and disturbance observer, Fig. 5, for the augmented plant (10) is then implemented using

$$\begin{bmatrix} \dot{\hat{\boldsymbol{x}}} \\ \dot{\hat{\boldsymbol{x}}}_{\boldsymbol{d}} \end{bmatrix} = \begin{bmatrix} A - L_x C & B_d C_d \\ -L_d C & A_d \end{bmatrix} \begin{bmatrix} \hat{\boldsymbol{x}} \\ \hat{\boldsymbol{x}}_{\boldsymbol{d}} \end{bmatrix} + \begin{bmatrix} B \\ 0 \end{bmatrix} \boldsymbol{u} + \begin{bmatrix} L_x \\ L_d \end{bmatrix} \boldsymbol{y}; \quad \hat{\boldsymbol{d}} = C_d \boldsymbol{x}_{\boldsymbol{d}}, \tag{11}$$

where the $\hat{[\,]}$ states are the estimate of the respective state. The so far unknown observer gain $L = [L_x^T, L_d^T]^T \in \mathbb{R}^{(10+6)\times(10+6)}$ is found by solving a Ricatti equation using only the virtual noise $\boldsymbol{w}$ as input to the augmented system (10). The solution of the Ricatti equation will be an optimal linear quadratic estimator (LQE) with respect to the plant and the covariance matrices of the measurement noise V and the virtual disturbance noise W.

3.2 Disturbance compensation

The disturbance compensation will be performed using the estimation of the disturbance. The inverse system, thus the input/output linearization is used to estimate the input needed to compensate the disturbance. The disturbance compensation is based on the linearized MBS (6). The dilemma with the actuator is, that only two control goals are achievable, because the dimension of $\boldsymbol{u}$ is only two. Therefore, the goal of the disturbance is set to be $\boldsymbol{y}_{\boldsymbol{ctrl}} = [z_c, \beta_c]^T = \boldsymbol{h}(\overline{\boldsymbol{q}}_a, \overline{\boldsymbol{q}}_u)$, which shall be compensated with the two inputs $\boldsymbol{u} = [F_c, T_c]^T$. Only the basic idea of the inverse dynamics will be given here, due to the limitation in space, for details see [9]. The main idea for the control of under actuated MBS is the separation of the generalised coordinates $\overline{\boldsymbol{q}}$ in an actuated part $\overline{\boldsymbol{q}}_a = [r_c, \varphi_c]^T$ and and unactuated part $\overline{\boldsymbol{q}}_{\boldsymbol{u}} = [x_b, z_b, \beta_c]^T$. In the linear MBS represented by equation (6) the actuated coordinates $\overline{\boldsymbol{q}}_{\boldsymbol{a}}$ and their derivatives are replaced by the output $\boldsymbol{y}_{ctrl}$ using the inverse of the output function $\overline{\boldsymbol{q}}_{\boldsymbol{a}} = \boldsymbol{h}^{-1}(\boldsymbol{y}_{\boldsymbol{ctrl}}, \boldsymbol{q}_{\boldsymbol{u}})$ and its derivatives, which is analytically possible for a linear system. The resulting representation of the MBS is than split in two parts:

$$\begin{aligned} \ddot{\boldsymbol{y}} &= \boldsymbol{f}_y(\boldsymbol{y}_{\boldsymbol{ctrl}}, \dot{\boldsymbol{y}}_{\boldsymbol{ctrl}}, \boldsymbol{q}_{\boldsymbol{u}}, \dot{\boldsymbol{q}}_{\boldsymbol{u}}) + \boldsymbol{g}_{\boldsymbol{yu}} \cdot \boldsymbol{u} + \boldsymbol{g}_{\boldsymbol{yd}} \cdot \boldsymbol{d} \\ \ddot{\boldsymbol{q}}_u &= \boldsymbol{f}_u(\boldsymbol{y}_{\boldsymbol{ctrl}}, \dot{\boldsymbol{y}}_{\boldsymbol{ctrl}}, \ddot{\boldsymbol{y}}_{\boldsymbol{ctrl}}, \boldsymbol{q}_{\boldsymbol{u}}, \dot{\boldsymbol{q}}_{\boldsymbol{u}}, \boldsymbol{u}, \boldsymbol{d}). \end{aligned} \tag{12}$$

The first part of (12) describes the dynamics of the output $\boldsymbol{y}$ and the second part describes the dynamics of the unactuated coordinates $\boldsymbol{q_u}$. The first part of (12) has to be inversed in order to calculate the input $\boldsymbol{u}$ with the given desired output $\boldsymbol{y} \rightarrow \boldsymbol{y}^* \equiv 0$ and the estimate of the disturbance $\boldsymbol{d} \rightarrow \widehat{\boldsymbol{d}}$. Note that $\boldsymbol{g_{yu}}$ has to have full rank for the inversion to work. The dynamics of the unactuated coordinates $\boldsymbol{q_u}$ has to be simulated online to achieve a consistent control input $\boldsymbol{u}$.

4 SIMULATION

The simulation shown in this paper is a "worst-case" scenario simulation of a lift ride, where each guide rail of the rope-free PTS is perturbed. This perturbation of the rails results in the motion of the mounting point B_s of the bucket as shown in Fig. 6(a). The motion at the point B_s is transmitted through the springs and dampers and results in force and torque acting at point B_s as shown in Fig. 6(b), in order to be able to compare the disturbance $\boldsymbol{d}$ with its estimate $\widehat{\boldsymbol{d}}$. The linearized model (8) was achieved using the steady-sate $\boldsymbol{q}^s = \left[\boldsymbol{r_{Cb}^{O}}^T, 0, 0.963, 0\right]^T$ and its derivative $\dot{\boldsymbol{q}}^s = [0,0,0,0,0]^T$. The system matrices for each of the three disturbances are to be assumed the same and are given by

$$A_{d,i} = \begin{bmatrix} 0 & \omega \\ -\omega & 0 \end{bmatrix};\ G_i = \begin{bmatrix} 0 \\ 1000 \end{bmatrix}; C_{d,i} = [10^5 \quad 0\ ], \text{for } i = 1,2, \tag{13}$$

where ω is chosen to be 45, thus the disturbance generator displays a fast sinusoidal vibration. The large scaling factors in G_i and $C_{d,i}$ display the large force and torque, which are needed to move the cabin. The choice of the disturbance generator (13) is one of the design parameters of the disturbance estimation. Another design parameter are the covariance matrices of the measurement noise $\boldsymbol{v}$ and the disturbance noise $\boldsymbol{w}$ for the LQE design. The covariance matrices were here for simplicity and missing information of the measurement noise chosen to be identity matrices with respective sizes and a scaling factor

$$W = 10^6 \cdot I_3\ ;\ V = \ 10^{-4} \cdot I_5. \tag{14}$$

The choice of the covariance matrices (14) leads to a quit optimal estimation of the disturbance, due to the high trust in the output $\boldsymbol{y}$ determined by the small covariance V. The observer gain L of (11) is than found by solving the Ricatti equations in MATLAB by using the command `lqe`. The parameters have been chosen as shown in Table 1 and the damping parameters have been chosen to have the numeric value of the square route of its respective stiffness.

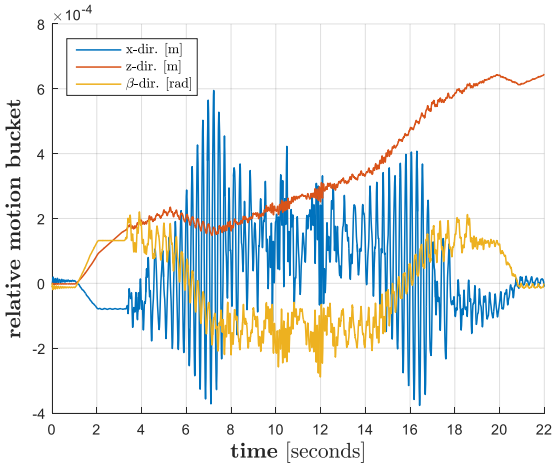

(a) Relative motion of bucket at B_s.

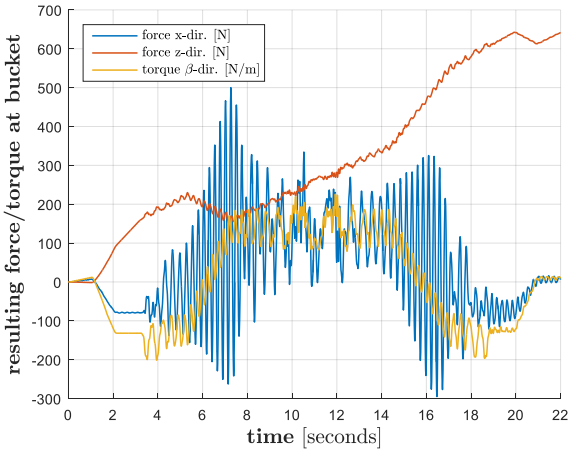

(b) Resulting force and torque at B_s.

Figure 6 Pre-simulated motion of the bucket (a), using deviated rail profiles for each guidance rail. The resulting force and torque at B_s (b) conveyed through the spring damper system.

The result of the disturbance compensation is shown in the Fig. 7 by comparing the output $\boldsymbol{y_{ctrl}}$ without to the output with disturbance compensation. The improvement with the disturbance compensation is clearly visible in Fig 7. Fig. 8 shows the actually more interesting feature with respect to the vibration damping the actual acceleration inside the cabin filtered by the human sensitivity function from the ISO-Norm [12]. The improvement in the direction of the controlled output is again clearly visible in Fig. 8. Fig. 8 also displays the restriction of the chosen control output $\boldsymbol{y_{ctrl}}$ in combination with the two actuators, thus the input $\boldsymbol{u}$. The control scheme those not directly compensate any motion in the x-direction of the cabin, as visible in Fig. 8(b), because only two goals can be met with the given structure of the controller.

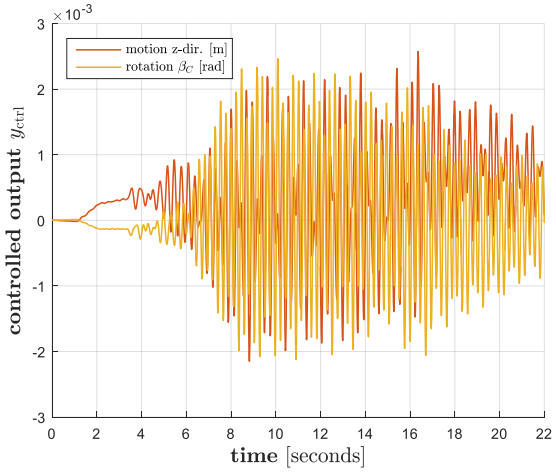

(a) Without disturbance compensation.

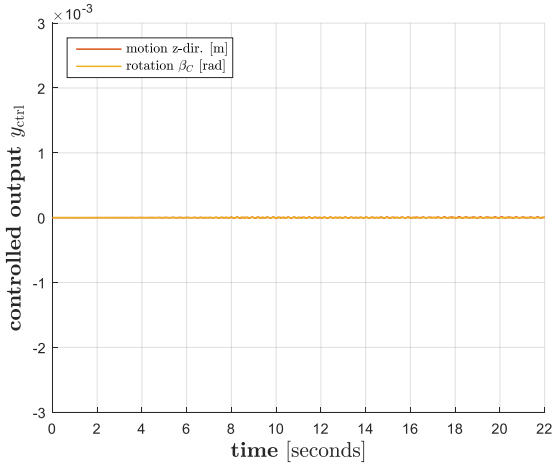

(b) Linear disturbance compensation.

Figure 7 Controlled output y_{ctrl} without (a) and with linear disturbance compensation (b).

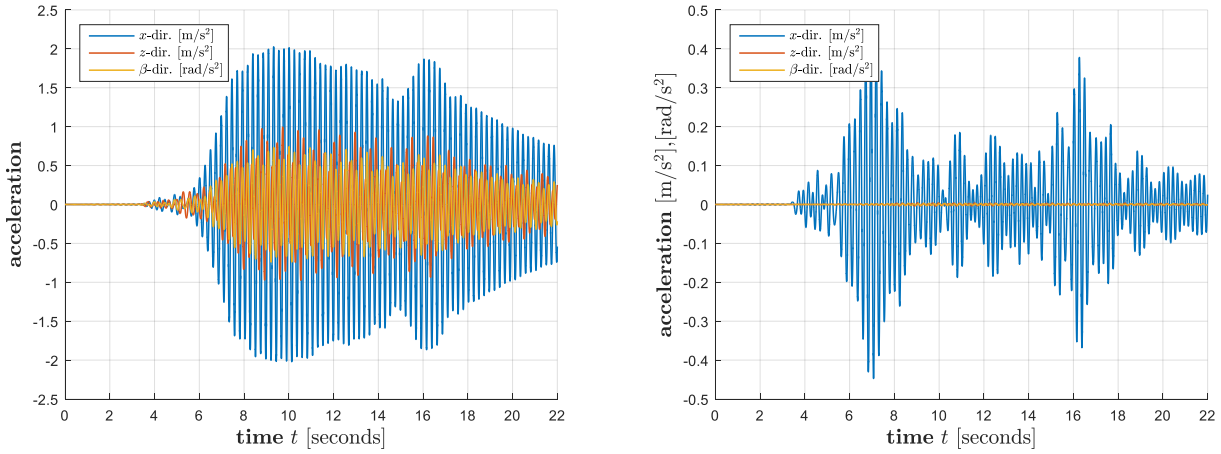

(a) Without disturbance compensation. **(b) Linear disturbance compensation.**

Figure 8 Acceleration of controlled output and acceleration in x-direction of cabin filtered with the respective human sensitivity function [12].

5 CONCLUSION AND OUTLOOK

This paper presented a control strategy for the active cabin vibration damping of a rope-free PTS. The control strategy is based on the combination of disturbance compensation with estimation of the disturbance, which in general cannot be measured directly. The first simulation of the control strategy with a simplified two-dimensional model of the rope-free PTS shows promising results and suggests further investigation of the control technique. The many tuneable parameters, as the assumed disturbance generator model and the covariance matrices of the LQE design, includes room for the adjustment to the real world system.

The main limitation of the proposed control scheme is not the control strategy, but the actuator itself, which is not designed to damp vibrations in x-direction. In order to damp vibrations in the x-direction of the cabin an additional actuator input has to be designed. Another way to improve the control concept is to incorporate the real goal in the control output function $\boldsymbol{h}$, thus the damping of the acceleration inside the cabin. The used control output $\boldsymbol{y_{ctrl}}$ achieves this indirectly by damping all motions to zero, but a less restrictive damping rule might be better suited for the task. The model consisting only of mounting frame and bucket completely obviously omits the sledge and therefore neglects all feedback caused by the actuators to the sledge. In order to verify the model design further simulations including the sledge will be necessary.

Table 1 Parameter and initial distances for the simulation

Parameter	Value	Parameter	Value
Mass [kg]		**Inertia [kg m²]**	
Cabin	$\boldsymbol{m_c = 1000}$	Cabin	$\boldsymbol{I_c = 500}$
Mounting	$\boldsymbol{m_b = 200}$	Mounting	$\boldsymbol{I_b = 50}$
Actuator	$\boldsymbol{m_A = 2}$	Actuator	$\boldsymbol{I_A = 0.075}$
Initial distances [m]			
$\boldsymbol{B_s \rightarrow C_b}$	$\boldsymbol{r_{Cb}^{Bs} = [0.165, -0.6]^T}$	$\boldsymbol{O \rightarrow B_s}$	$\boldsymbol{r_{Bs}^{O} = [0, 0]^T}$
$\boldsymbol{C_b \rightarrow B_0}$	$\boldsymbol{r_{B0}^{Cb} = [0.75, -0.3]^T}$	$\boldsymbol{P_0 \rightarrow C_c}$	$\boldsymbol{r_{Cc}^{P0} = [0, 0.9]^T}$
$\boldsymbol{B_0 \rightarrow B_1}$	$\boldsymbol{r_{B1}^{Bs} = [-0.5, 0]^T}$	$\boldsymbol{P_0 \rightarrow P_1}$	$\boldsymbol{r_{P1}^{P0} = [-0.5, 0]^T}$
$\boldsymbol{B_0 \rightarrow B_2}$	$\boldsymbol{r_{B2}^{Bs} = [0.5, 0]^T}$	$\boldsymbol{P_0 \rightarrow P_2}$	$\boldsymbol{r_{P2}^{P0} = [0.5, 0]^T}$
Translational Stiffness [N/m]		**Rotational Stiffness [N/rad]**	
Point $\boldsymbol{B_s}$ $\boldsymbol{(x)}$	$\boldsymbol{k_{xB} = 10^6}$	Point $\boldsymbol{B_s}$	$\boldsymbol{k_{\beta B} = 10^6}$
Point $\boldsymbol{B_s}$ $\boldsymbol{(z)}$	$\boldsymbol{k_{zB} = 10^6}$		
Actuator	$\boldsymbol{k_{rc} = 2 \cdot 10^6}$	Actuator	$\boldsymbol{k_{\varphi c} = 2.2 \cdot 10^6}$

REFERENCES

[1] R. Madoński and P. Herman, “Survey on methods of increasing the efficiency of extended state disturbance observers" (eng). *ISA transactions*, Vol. 56, 18–27 (2015).

[2] P. Hippe and J. Deutscher, *Design of Observer-based Compensators: From the Time to the Frequency Domain*: Springer London. London (2009).

[3] R. E. Kalman, “A New Approach to Linear Filtering and Prediction Problems". *Transactions of the ASME-Journal of Basic Engineering*, Vol. 82, No. Series D, 35–45 (1960).

[4] Z. Gao, “Active disturbance rejection control: a paradigm shift in feedback control system design" *American Control Conference, 2006: 14 - 16 June 2006, [Minneapolis, MN]*: IEEE Operations Center, Piscataway, NJ, 7 pp (2006).

[5] M. Ramírez-Neria, H. Sira-Ramírez, R. Garrido-Moctezuma, and A. Luviano-Juárez, “Linear active disturbance rejection control of underactuated systems: the case of the Furuta pendulum" (eng). *ISA transactions*, Vol. 53, No. 4, 920–928 (2014).

[6] W. Schiehlen, “Multibody System Dynamics: Roots and Perspectives". *Multibody System Dynamics*, Vol. 1, No. 2, 149–188 (1997).

[7] Jonas Missler, Thomas Ehrl, Benedikt Meier, Stefan Kaczmarcyk, Oliver Sawodny, “Modelling of a rope-free Passenger Transportation System for Active Cabin Vibration Damping". *6th Lift and Escalator Symposium*, Vol. 2016 (2016).

[8] W. Schiehlen and P. Eberhard, *Applied Dynamics*: Springer International Publishing. Cham, s.l. (2014).

[9] R. Seifried, *Dynamics of Underactuated Multibody Systems*: Springer International Publishing. Cham (2014).

[10] C. I. Byrnes and A. Isidori, “Local stabilization of minimum-phase nonlinear systems". *Systems & Control Letters*, Vol. 11, No. 1, 9–17 (1988).

[11] A. Isidori, *Nonlinear Control Systems II*, 1st ed.: Springer London. Guildford, Surrey (2013).

[12] *Human response to vibration - Measuring instrumentation*, ISO 8041-1 (2005).

BIOGRAPHICAL DETAILS

Jonas Missler received his bachelor's degree in Engineering Cybernetics from the University of Stuttgart, Germany. He also obtained his master's degree in Engineering Cybernetics from the University of Stuttgart. Since 2015, he is working towards his Ph.D. at the Institute for System Dynamics at the University of Stuttgart. His current research interests are the developing of an active damping concept and the respective control scheme for rope-free PTS.

Thomas Ehrl, Mechanical Design Engineer (degree in 1994), Part-time PhD student with the School of Science and Technology of The University of Northampton. Professional career started in 1994. Since 4/2008 with thyssenkrupp Elevator: Head of Research & Innovation Center of TKE Innovation GmbH, Pliezhausen; Engineering Training Manager at Corporate Level of TKE AG; Manager R&D Project Standards at Corporate Level of TKE AG. Interests: Travelling, sports, soccer, music, vintage English motor cycles, model building, photography.

Benedikt Meier received his Diploma in Mechanical Engineering from the University of Hannover, Germany. In 1992, he obtained his doctorate in Cold Testing of combustion engines. In thyssenkrupp Elevator AG, he is leading the Global Project Management Office (PMO). Since July 2015, he serves as Visiting Professor in the School of Science and Technology at the University of Northampton. His expertise is in the area of horizontal and vertical transportation and material handling systems. In addition, he is an internationally recognized expert in Project and Program Management. Professor Meier has published several journal and international conference papers in his area of expertise.

Stefan Kaczmarczyk has a master's degree in Mechanical Engineering and he obtained his doctorate in Engineering Dynamics. He is Professor of Applied Mechanics and Postgraduate Programme Leader for Lift Engineering at the University of Northampton. His expertise is in the area of applied dynamics and vibration with particular applications to vertical transportation and material handling systems. He has been involved in collaborative research with a number of national and international partners and has an extensive track record in consulting and research in vertical transportation and lift engineering. Professor Kaczmarczyk has published over 90 journal and international conference papers in this field. He is a Chartered Engineer, being a Fellow of the Institution of Mechanical Engineers, and he has been serving on the Applied Mechanics Group Committee of the Institute of Physics.

Professor Oliver Sawodny received his Dipl.-Ing. degree in electrical engineering from the University of Karlsruhe, Karlsruhe, Germany, in1991 and his Ph.D. degree from the University of Ulm, Ulm, Germany, in 1996. In 2002, he became a Full Professor at the Technical University of Ilmenau, Ilmenau, Germany. Since 2005, he has been the Director of the Institute for System Dynamics, University of Stuttgart, Stuttgart, Germany. His current research interests include methods of differential geometry, trajectory generation, and applications to mechatronic systems. He received important paper awards in major control application journals such as Control Engineering Practice Paper Prize (IFAC, 2005) and IEEE Transaction on Control System Technology Outstanding Paper Award (2013).

Why PESSRAL is not PESS

Tijmen Molema

buikslotermeerplein 381, 1025XE, The Netherlands

Liftinstituut, tijmen.molema@liftinstituut.com

Keywords: PESSRAL, PESS, Safety

Abstract. The lift industry is quite old-fashioned in electric / electronic / programmable electronic (E/E/PE) safety: they used the electric safety chain for more than 30 years. However, since the EN 81-1/2 A1: 2005 amendment, the standard allows to use programmable electronics for safety systems (PESS). Also, the code committee decided to implement a subset of the leading norm (IEC 61508) into EN 81 in order to decrease the difficulty and increase the implementation speed: PESSRAL (Programmable Electronic System in Safety Related Applications for Lifts) was born. However, due to cherry picking and skipping the basics the old and even the newest code (EN-81-20/50) makes it possible to create unsafe systems. Where are the potential risks?

1 LEADING NORM

The IEC 61508 itself consists of 7 different pieces with a total of more than 500 pages. It describes the complete path to follow when creating an E/E/PE safety device. It contains calculations, assumptions, design strategies, risk analyses, and descriptions of quality systems. It results in a SIL (safety integrity level) which is a mathematical number expressing the safety of the system. All of this documentation is needed to end up in a safe system. In contrast: EN 81-20/50 uses 11 pages and claims to be a full package.

2 SYSTAMATIC CABABILITY

The entire process flow for making a PESS is described in a separate part of the standard, the 61508-1. By a clear way of working and project management we try to minimize systematic failures in a system. There are clear demands and this results in a SC (systematic capability) value. Techniques which can be used are e.g. project management, documentation, structured design and modularization as well as the SC, as these techniques are not demanded or described in EN 81-20. Projects without proper management can contain major mistakes, and these are hard to spot.

3 RISK ANALYSIS

For safety software, SIL (safety integrity level) is used to measure safety. It is a mathematical number expressing the safety of the system. For example: SIL 3 has an average chance of failure between 10^{-9} and 10^{-8} or 10^{-5} to 10^{-4} an hour depending on the demanded rate. Normally you have to perform a risk analyses in order to determine the needed SIL rate. The EN81-1/2+A3 and EN 81-20/50 have already performed this risk analyses in it and ask for SIL ratings. This way there is no need for a risk analyses anymore, which creates uniformity in the systems of competitors. However; a risk analyses gives insight in the project and influences the design. This is mandatory in IEC 61508 procedure, but not in EN 81-1/2 and EN 81-20.

4 DEMAND

So a SIL level is available, but it is not clear which SIL level we have to use exactly: the standard describes 2 types of SIL systems, high demand and low demand systems. Each of them have their own requirements. It is not clear by the EN81 if we are working in high or low demand. The difference in demand rate between these is mathematically a factor of 10.000 failures / hour. Low demand is explained in IEC 61508-4 as "where the safety function is only performed on demand, in order to transfer the EUC (Equipment under Control) into a specified safe state, and where the frequency of demands is no greater than one per year". For a lift, we do not use the over speed governor more than once a year, so is it than low demand? This is necessary to know because it gives a difference in the calculated safety by a factor of 10.000. It is not set clearly in the standard. However the IEC-62061 states that machines shall fulfill high demand. Most of the certifying organizations are following this guideline. Unfortunately it is not set plainly in the EN 81-20.

5 SAFE FAILURE FRACTION

When building a SIL 3 system, the relevant tables in EN 81-1/2+A3 and EN 81-50 require that a double channel system is mandatory. The main idea of this is 'when one channel fails, the other channel will put the system to a safe state'. IEC 61508 has the same principles, but there are some major discrepancies. IEC 61508 describes the model of SFF (Safe Failure Fraction): the fraction of failures which is safe and which is dangerous. For components where the failure mode cannot be predicted (like CPU's and other complex systems) the demands are set higher. Moreover, diagnostic software also increases the SFF. Due to the fact that EN81-20/50 demands a 2 channel system for SIL 3 it excludes the use of a totally fail-safe (SFF = 100%) 1 channel system and makes it possible to create a fail-unsafe (SFF << 90%) system. If every possible fault in a channel is directly dangerous (SFF = 0%), and if the fault remains undetected a second fault causes an unsafe system. This way, PESSRAL solutions can be less safe than the fault tree analyses present in the EN 81-20.

6 COMMON CAUSE

Due to not performing a risk analyses and the demand for 2 channels for SIL 3, a new difficulty occurs. By demanding 2 channels without any further specification it becomes possible to build 2 identical channels. These identical channels introduce the risk to fail at the same time due to the same error (common cause). Typical errors are a slightly to very low supply voltage, design faults inside a CPU, or temperature. When working with multiple channels, the common cause errors are the largest part of the total. I will demonstrate this with an example.

You can compare it with throwing a dice: by throwing a 1 you will lose: your chance of losing is exactly 1/6. To decrease this chance of losing you can add another dice, now you need two ones to lose the game. When calculating the chance of losing, we do 1/6 * 1/6 = 1/36. Now we introduce a common cause fault in this "system": a single fault which influences both channels (the dices). Due to the fact that on the other side of the dice the number "6" is represented, and for painting 6 dots we need slightly more paint. More paint means also more weight, and two opposite sides on a dice always give a total of 7. Due to this faulty design the chance of throwing a 1 is bigger than the other numbers. The chance of a double one is also bigger than the chance of another double combination. We assume that the change of throwing a 1 is 5% bigger; this value is token from the IEC-61508. The change of throwing one 1 is 1/6, a 5% higher change for one 1 is 1/6 + 1/6 * 1/20 comes to 7/40. The total change of throwing 2 times a 1 is now 7/40 * 7/40 = 49/1600, or +- 3%. As comparison, 1/36 is 2,8%.

The standard doesn't care which faults can be a common cause: all faults has to be taken into consideration as a possible common cause. Due to this, I can simplify the calculation: Take the dangerous fault and multiply it with the common cause factor. For the dices this will mean that we

have the 1/6 (fault change of 1 channel) multiplied by 1/20: a factor of 1/120 is added as common cause, or 0,8%. We end up with a fault change of 2,8 + 0,8 = 3,6%. It is bigger than the full calculation, but it is on the safe side and we considered all possible common causes.

For this system the impact is still relatively small. However the fault chance of a PESS channel is a lot smaller: for example 10^{-9} Doing the same calculations, the two channel system has a chance of failing of 10^{-9}* 10^^-9 = 10^^-18. Now we calculate the common cause part: $5*10^{-2} * 10^{-9} .= 5*10^{-11}$ We can see clearly that the common cause part is way bigger than the single channel faults. If we have smaller failing chances in channels, than the common cause will become more important and be the dominant part of the safety calculations, as well as they are in real safety. EN 81 does not tackle this problem: the common cause risk is not described, there are no techniques for common cause avoidance described, and nothing is calculated.

7 DIAGNOSTIC TECHNIQUES

EN 81-20 cherry picks a number of techniques and states them as mandatory. There is no calculation needed anymore (EN 81-50 states that IEC 61508-6, which explains the calculations, is not needed for understanding). IEC 61508 gives a large number of options; the most suitable technique can be chosen for the system. It can happen that completely non-relevant techniques are demanded, where other techniques are quite more useful. For example; there are no demands for sensors in the lift standard, but when we use a CLPD (complex logic programmable device) there are still demands for RAM checks and watchdogs; this is not right according IEC 61508. Also, we cannot check if our diagnostics are good enough. Normally DC (diagnostic coverage) has a direct influence on the SFF (safe failure fraction), and so on the entire safety calculation of the system.

8 CALCULATIONS

The backbone of IEC 61508 are the underlying calculations. By looking at all components FIT (failure in time) rates and design, a calculation of the chance of failure can be made. The calculated numbers should be in line with the SIL rate. FMEA (Failure Mode Effect Analyses) on components and DC in order to improve the SFF ends up in a safer system. IEC 61508 has demands on the SFF which needs to be met. The calculation is the theoretical basis, it gives insight in the weakest points of the system and proves that the system is safe enough. This calculation is not needed for EN 81, by fulfilling all demands you are done. These demands describe techniques only, but does not give any numbers. There is no check if the system is “safe enough”. It is possible to end up with a mathematical unsafe system.

For example: I can use two really bad relays parallel. When they fail once in every 10 times, they will both fail at the same time every 100 times (excluding common cause!). It still fulfills EN81-20 (double channel with diagnostics): I can detect that both relays are failing. However: I cannot act on it anymore. When we calculate the failure rates for the system with IEC 61508, we will directly find out that the relays are not good enough for this system: the FIT (failure in time) values will be devastating for the PFH (Product Failure / Hour). Due to the calculation, bad components are filtered out.

9 TESTING

Every system needs testing after development: there are always unforeseen problems which are filtered out during the test phase. Of course a PESSRAL system will be tested, but what test strategy is the proper one? Known that most of the industry has no practical experience with safety software and there are no test strategies mandatory or even mentioned in the standard. Most commonly known test method is black- / white box testing: it is a basic way of screening a system. It is usable for

electric- and mechanical systems. When creating PESS, the system is a full black box: However, IEC 61508 can also ask for traceability of the requirements, full modeling, software simulation and performance testing. Also there is no test procedure or awareness for common cause faults in the lift norm.

10 PROOF TEST INTERVAL

The lifetime of a system is not considered. Due to the fact that periodical inspection on PESS systems is almost impossible, a lifetime must be specified. Diagnostics in the system also cannot detect every possible fault, the DC is always smaller than 100%. Normally PESS systems have a “proof test interval”. The meaning of this proof test is to detect the normally undetected errors. EN 81 does not require this. This allows a system to build up an endless amount of errors and gives the possibility to end up with a dangerous fault.

11 DISCUSSION

At this moment, only a small amount of lifts work with PESS. For the ones that work, there are no major failures yet. PESS is possible since the first amendment of EN 81-1/2 in 2005. We do not know how many installations are in the field today, so we cannot determine why there were no failures. There are some possible explanations that can explain the fact that we did not have any accidents:

1. When making something revolutionary, a company must be absolutely sure that it is safe: otherwise the product will not be accepted in the market by the costumer. For PESSRAL, most lift company’s want to be absolutely sure that after several years it still works: so endurance tests will probably be done. This is a powerful testing method.
2. There are not that much PESSRAL systems in the world: most lifts have a long lifetime and controls are not regularly changed. Also the development of PESSRAL has just started: there are not that much PESSRAL systems on the market. Most of them are still in development.
3. The major certification bodies also perform tests on PESS systems. They have their own demands for testing, or will ask for a calculation. Certification bodies also want safe systems, and most of them know how to perform the tests properly due to the experience with IEC 61508.
4. There is no guideline for reporting crashes, and we cannot be sure that we will hear about all crashes in the world including the cause.

The biggest problems of these possible explanations are the fact that they are not mandatory: there are no demands on test time, there is no requirement for experience in PESS for notified bodies. Also worldwide information about lift catastrophes does not exists related to this topic.

12 CONCLUSION

PESSRAL is not PESS: and this is not only due the absence of a lot of background information. The entire mathematical backbone is gone: we cannot calculate if the chance of failure of the system is right. This has a huge impact on the common cause faults. These are the most dangerous faults for a double channel system. Also the channels itself can be made out of unsafe components. The only way to check the system now is by testing, but testing strategies are not described. Until this moment of writing, there are no fatal accidents yet. However we cannot explain why they did not happen, or predict that they will not happen. In the end, it is possible to build unsafe systems with the rules of PESSRAL. For now we can only hope that lifts will stay safe, for the future we need EN 81-20 to change as quickly as possible.

BIOGRAPHICAL DETAILS

Tijmen Molema is a product specialist certification for Liftinstituut. His specialty is in software and electronics. He studied Electronic Engineering and Design at the Hogeschool Utrecht. He started in 2014 as a lift inspector, but quickly became a product specialist for all kind of electronic challenges.

His personal goal is to help the lift industry to leave the “old” relays systems, and lead it to a new and progressive market.

Liftinstituut is an independent Body which is specialized in product certification and surveys of hoisting equipment for goods and persons. Liftinstituut is therefore also notified by the Dutch authorities as Notified Body(0400) for the Lift directive (95/16/EC) and machine directive (2006/42/EC) for e.g. *lifting devices of persons or of persons and goods involving a hazard of falling from a vertical height of more than three meters hoisting and logic controllers.*

In the USA Liftinstituut is also registered as AECO for Lifts (0842).